Nuclear symmetry energy constraint from isospin diffusion with INDRA-FAZIA

Caterina Ciampi

GANIL

for the INDRA-FAZIA collaboration

European Nuclear Physics Conference
(EuNPC 2025)

Caen, France
September 22nd - 26th, 2025

Nuclear Equation of State (nEoS): Thermodynamic description of nuclear matter.

Nuclear Equation of State (nEoS): Thermodynamic description of nuclear matter.

$e(\rho, \delta) = e(\rho) + S(\rho)\delta^2$ → Largest uncertainties on **symmetry energy** $S(\rho)$

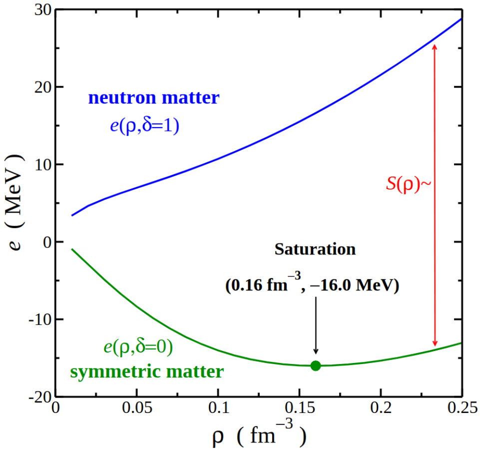

Nuclear Equation of State (nEoS): Thermodynamic description of nuclear matter.

$e(\rho,\delta) = e(\rho) + S(\rho)\delta^2$ $\longrightarrow$ Largest uncertainties on **symmetry energy** $S(\rho)$

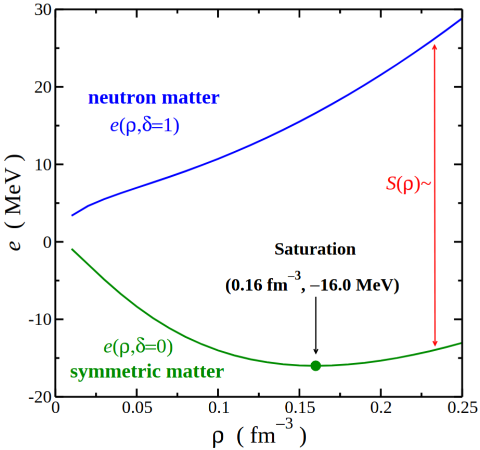

Isospin transport phenomena:
sensitive probe to study $S(\rho)$

$$\mathbf{j}_n - \mathbf{j}_p \propto S(\rho)\nabla\delta + \delta\frac{\partial S(\rho)}{\partial\rho}\nabla\rho$$

Outline

Nuclear Equation of State (nEoS): Thermodynamic description of nuclear matter.

$e(\rho,\delta) = e(\rho) + S(\rho)\delta^2$ → Largest uncertainties on **symmetry energy** $S(\rho)$

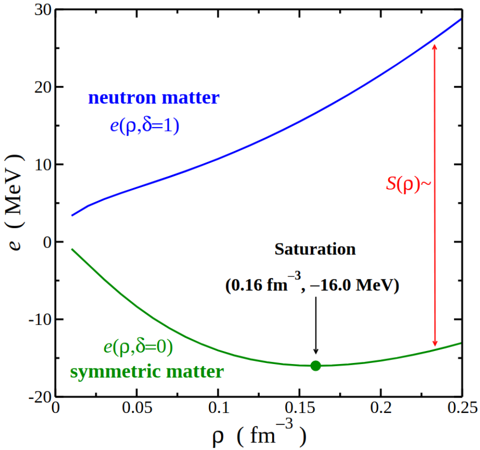

Isospin transport phenomena: sensitive probe to study $S(\rho)$

$$\mathbf{j}_n - \mathbf{j}_p \propto S(\rho)\nabla\delta + \delta\frac{\partial S(\rho)}{\partial\rho}\nabla\rho$$

Isospin diffusion: driven by isospin gradient in the system, leads to isospin equilibration.

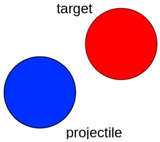

Nuclear Equation of State (nEoS): Thermodynamic description of nuclear matter.

$e(\rho,\delta) = e(\rho) + S(\rho)\delta^2$ $\longrightarrow$ Largest uncertainties on **symmetry energy** $S(\rho)$

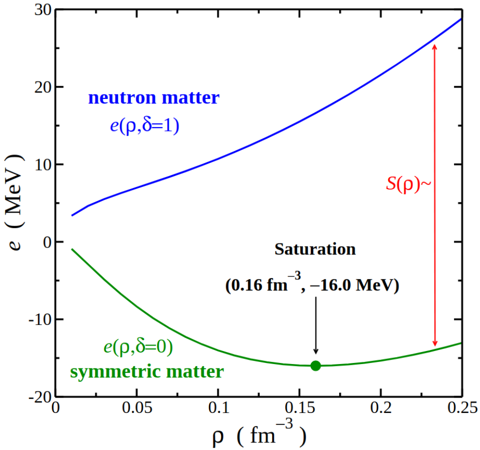

Isospin transport phenomena: sensitive probe to study $S(\rho)$

$$\mathbf{j}_n - \mathbf{j}_p \propto S(\rho)\nabla\delta + \delta\frac{\partial S(\rho)}{\partial\rho}\nabla\rho$$

Isospin diffusion: driven by isospin gradient in the system, leads to isospin equilibration.

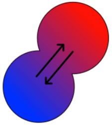

Nuclear Equation of State (nEoS): Thermodynamic description of nuclear matter.

$$e(\rho,\delta) = e(\rho) + S(\rho)\delta^2$$ → Largest uncertainties on **symmetry energy** $S(\rho)$

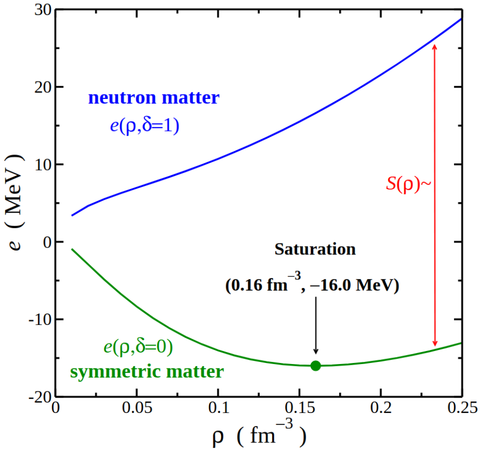

Isospin transport phenomena: sensitive probe to study $S(\rho)$

$$\mathbf{j}_n - \mathbf{j}_p \propto S(\rho)\nabla\delta + \delta\frac{\partial S(\rho)}{\partial\rho}\nabla\rho$$

Isospin diffusion: driven by isospin gradient in the system, leads to isospin equilibration.

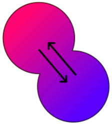

Nuclear Equation of State (nEoS): Thermodynamic description of nuclear matter.

$e(\rho,\delta) = e(\rho) + S(\rho)\delta^2$ → Largest uncertainties on **symmetry energy** $S(\rho)$

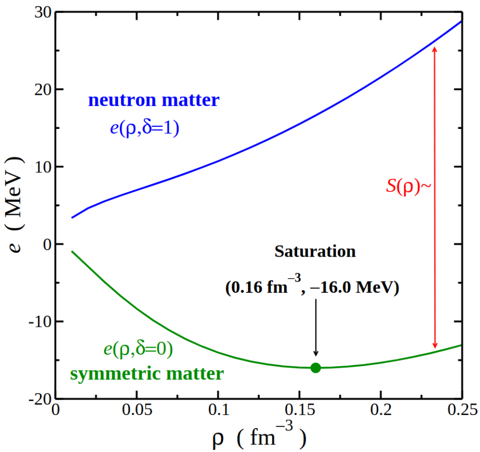

Isospin transport phenomena: sensitive probe to study $S(\rho)$

$$\mathbf{j}_n - \mathbf{j}_p \propto S(\rho)\nabla\delta + \delta\frac{\partial S(\rho)}{\partial\rho}\nabla\rho$$

Isospin diffusion: driven by isospin gradient in the system, leads to isospin equilibration.

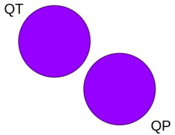

The INDRA-FAZIA setup
Exploring isospin dynamics in heavy ion collisions

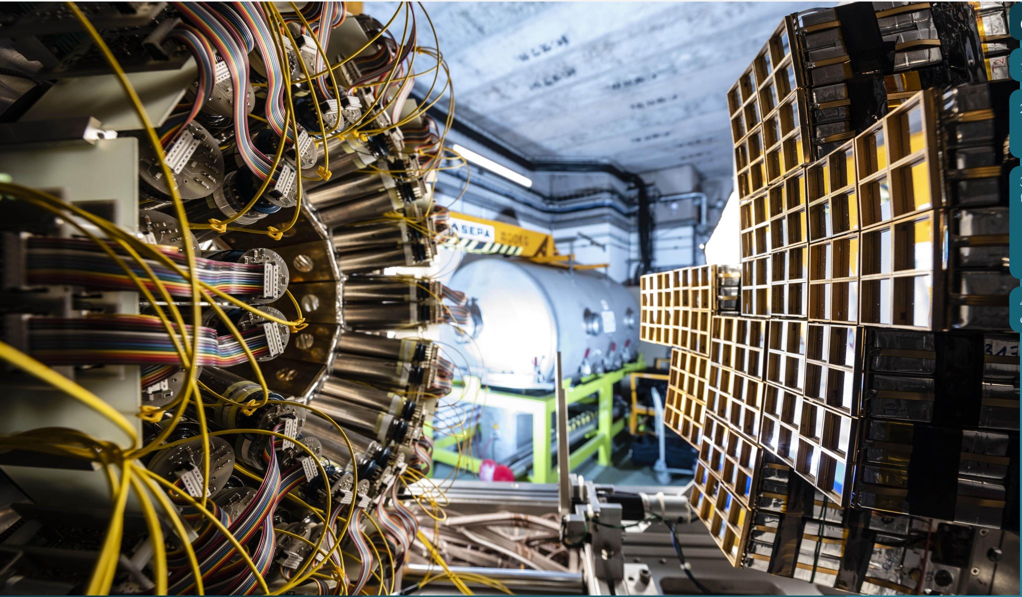

Outline

FAZIA
Forward-angle A and Z Identification Array

State of the art of ion identification in the Fermi energy domain

Covers the most forward polar angles for (Z, A) identification of QP-like fragments

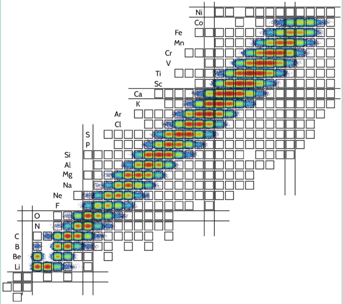

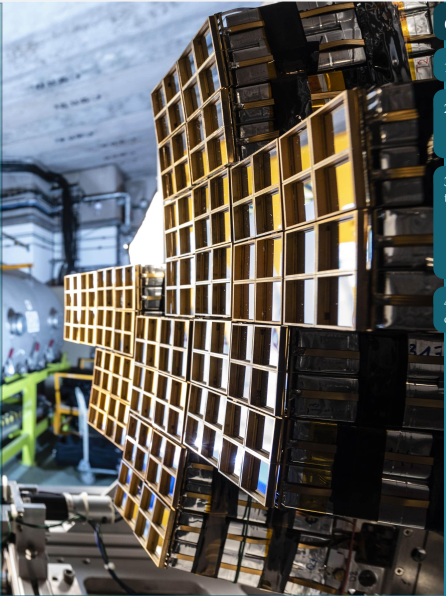

Outline

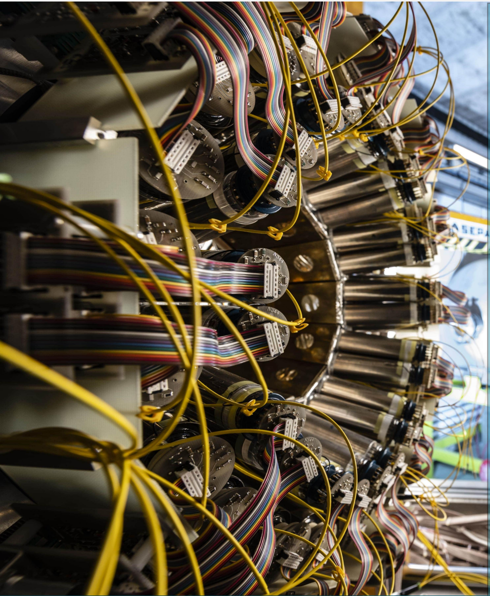

INDRA
Identification de Noyaux et Détection avec Résolutions Accrues

Offers large solid angle coverage (~80% of 4π) with high granularity

Provides a good global event reconstruction

Build global variables for reaction centrality estimation

Outline

The INDRA-FAZIA setup

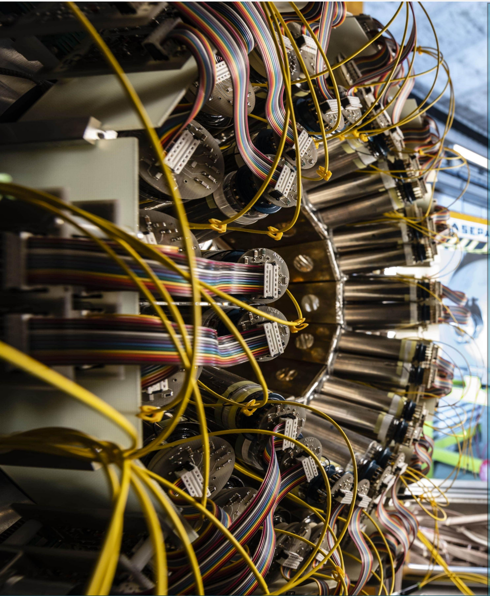

INDRA

Identification de Noyaux et Détection avec Résolutions Accrues

Offers large solid angle coverage ($\sim$80% of 4π) with high granularity

Provides a good global event reconstruction

Build global variables for reaction centrality estimation

Outline

Centrality-related observable $X \longleftrightarrow$ deduce the correspondence with b

(see J. D. Frankland et al., PRC104, 034609 (2021), R. Rogly et al., PRC98, 024902 (2018))

$\Rightarrow$ Need to model the conditional probability distribution: $\mathbf{P(X|b)}$

Step 1

Parametrize the $\mathbf{P(X|b)}$, taking into account both the mean value and the fluctuations

Centrality-related observable $X \longleftrightarrow$ deduce the correspondence with b

(see J. D. Frankland et al., PRC104, 034609 (2021), R. Rogly et al., PRC98, 024902 (2018))

$\Rightarrow$ Need to model the conditional probability distribution: $\mathbf{P(X|b)}$

Step 1

Parametrize the $\mathbf{P(X|b)}$, taking into account both the mean value and the fluctuations

Step 2

From the **inclusive** distribution $P(X)$, extract the $\mathbf{P(X|b)}$ parameters by fitting:

$$P(X) = \int_0^\infty P(b)\,\mathbf{P(X|b)}\,db \qquad P(b) = \frac{2\pi b}{1 + \exp\left(\frac{b-b_0}{\Delta b}\right)}$$

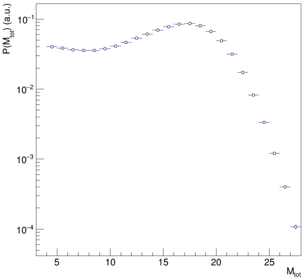

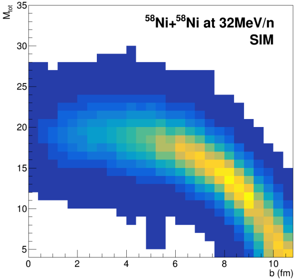

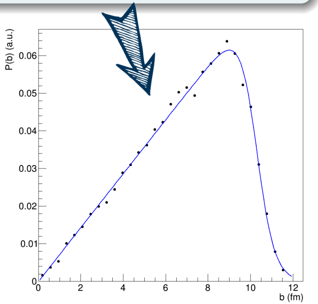

Centrality-related observable $X \longleftrightarrow$ deduce the correspondence with b

(see J. D. Frankland et al., PRC104, 034609 (2021), R. Rogly et al., PRC98, 024902 (2018))

$\Rightarrow$ Need to model the conditional probability distribution: $\mathbf{P(X|b)}$

Step 1

Parametrize the $\mathbf{P(X|b)}$, taking into account both the mean value and the fluctuations

Step 2

From the **inclusive** distribution $P(X)$, extract the $\mathbf{P(X|b)}$ parameters by fitting:

$$P(X) = \int_0^\infty P(b)\,\mathbf{P(X|b)}\,db \qquad P(b) = \frac{2\pi b}{1+\exp\left(\frac{b-b_0}{\Delta b}\right)}$$

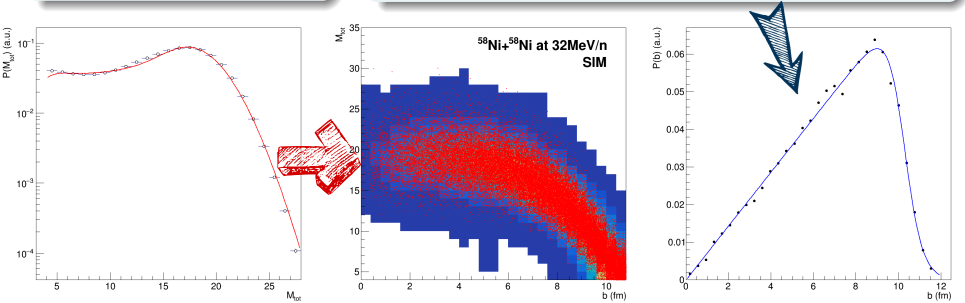

Impact parameter reconstruction

Basic structure of the method

Centrality-related observable $X \longleftrightarrow$ deduce the correspondence with b

(see J. D. Frankland et al., PRC104, 034609 (2021), R. Rogly et al., PRC98, 024902 (2018))

$\Rightarrow$ Need to model the conditional probability distribution: $\mathbf{P(X|b)}$

Step 1

Parametrize the $\mathbf{P(X|b)}$, taking into account both the mean value and the fluctuations

Step 2

From the **inclusive** distribution $P(X)$, extract the $\mathbf{P(X|b)}$ parameters by fitting:

$$P(X) = \int_0^\infty P(b)\,\mathbf{P(X|b)}\,db \qquad P(b) = \frac{2\pi b}{1+\exp\left(\frac{b-b_0}{\Delta b}\right)}$$

Step 3

Having the $\mathbf{P(X|b)}$, for each X selection we can evaluate:

$$P(b|x_1 < X < x_2) = \frac{\int_{x_1}^{x_2} P(b,X)\,dX}{\int_{x_1}^{x_2} P(X)\,dX} = \frac{\int_{x_1}^{x_2} P(X)\,P(b|X)\,dX}{\int_{x_1}^{x_2} P(X)\,dX} = \frac{\int_{x_1}^{x_2} P(b)\,\mathbf{P(X|b)}\,dX}{\int_{x_1}^{x_2} P(X)\,dX}$$

⚠ To obtain the impact parameter distribution, it is necessary to perform the fit on the most inclusive $P(X)$ distribution, for which the $P(b)$ above can be assumed.

Outline

Combined analysis of two Ni-Ni@32 MeV/nucleon datasets bearing complementary information:

INDRA-FAZIA dataset → ^{58,64}Ni+^{58,64}Ni at 32 MeV/nucl.
Includes the information on the *isospin content of the QP remnant*. Biasing trigger for semiperipheral collisions.

INDRA dataset → ^{58}Ni+^{58}Ni at 32 MeV/nucl.
Trigger $M_{\text{tot}} \geq 4$ → minimum bias, suitable for the application of the *impact parameter reconstruction method*.

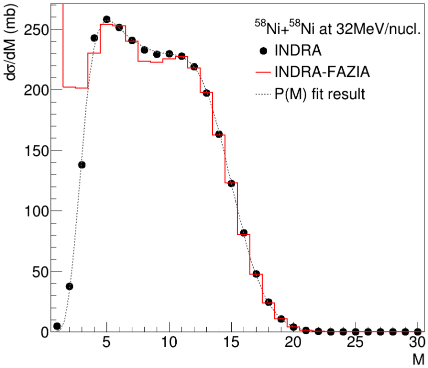

Combined analysis of two Ni-Ni@32 MeV/nucleon datasets bearing complementary information:

INDRA-FAZIA dataset → ^{58,64}Ni+^{58,64}Ni at 32 MeV/nucl.
Includes the information on the *isospin content of the QP remnant*. Biasing trigger for semiperipheral collisions.

INDRA dataset → ^{58}Ni+^{58}Ni at 32 MeV/nucl.
Trigger $M_{tot} \geq 4$ → minimum bias, suitable for the application of the *impact parameter reconstruction method*.

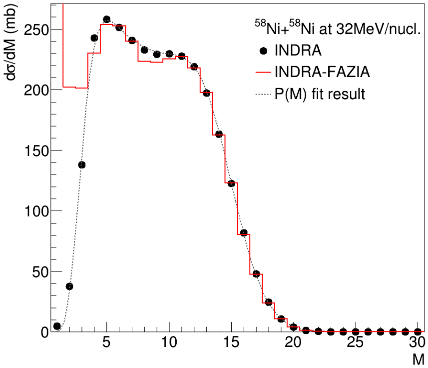

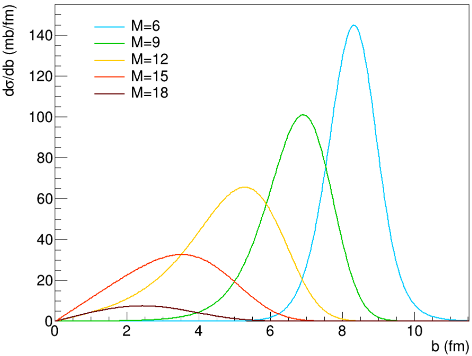

→ important role of **intrinsic fluctuations**: relatively different M selections populate partly (or entirely) superimposed b intervals

INDRA-FAZIA experimental data
Selection of the events

In view of producing the most general result, easily comparable with any theoretical prediction, we avoid a strictly exclusive analysis.

- No distinction among different output channels
- QP remnant selected as:
  1. fragment with largest Z in forward hemisphere
  2. if more than one with same Z, select largest $v_z^{\text{c.m.}}$
- Minimum size to consider a QP remnant: $Z_{QP} \geq 5$
  $\rightarrow$ include light products from very dissipative events

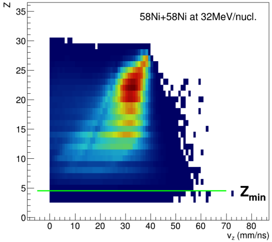

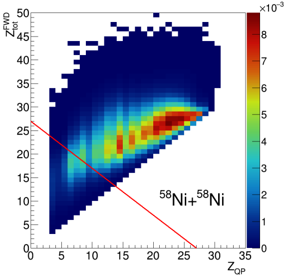

Light QP remnants $\rightarrow$ carefully check the completeness of the event to exclude those in which the heaviest fragment has been lost.

- The total undetected charge in the forward hemisphere should not exceed Z_{QP}
- Accept event if $Z_{QP} \geq 28 - Z_{tot}^{FWD}$
- We verified that by removing < 13% of events, the final result becomes stable against reasonable variations of Z_{QP}^{min}

Each event is assigned an impact parameter value randomly drawn from the b distribution associated with its corresponding M_{resc} value $\Rightarrow$ take into account the fluctuations

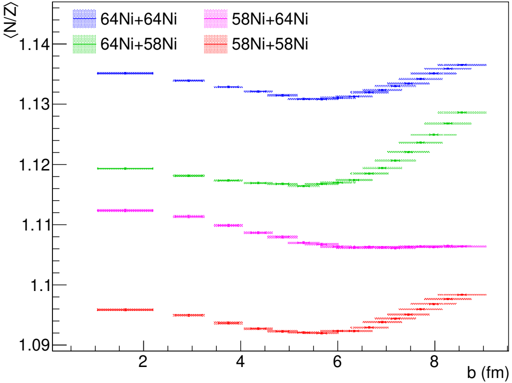

Model-independent $\langle N/Z \rangle$ for the QP remnant as a function of b for the four systems in the INDRA-FAZIA dataset

Clear effect of isospin equilibration down to the most central collisions:

- *peripheral*: similar result for reactions with same projectile
- *central*: $\langle N/Z \rangle$ depends on target, mixed systems tend to each other

Horizontal error bars: statistics + uncertainty on the estimation of b_0 in the $P(b)$ assumed for the impact parameter reconstruction method (affecting less central collisions to a greater extent).

Isospin transport ratio: can highlight the isospin diffusion effect, bypassing the effects acting similarly on the four systems (F. Rami et al., Phys. Rev. Lett. 84, 1120 (2000))

$$R(x) = \frac{2x_i - x_{AA} - x_{BB}}{x_{AA} - x_{BB}}$$

- $R(x) = \pm 1 \longrightarrow$ non equilibrated
- $R(x_{AB}) = R(x_{BA}) \longrightarrow$ full equilibration

where $A = {}^{64}$Ni, $B = {}^{58}$Ni, $i = AA, AB, BA, BB$ and x is an isospin sensitive observable.

Model-independent isospin transport ratio R(⟨N/Z⟩) for the QP remnant as a function of the impact parameter b

Regular behavior towards equilibration for increasing centralities (full equilibration is not achieved).

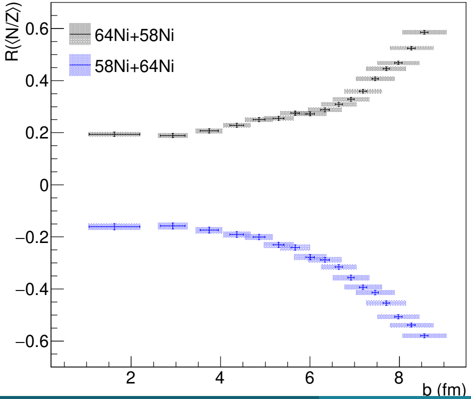

Isospin transport ratio: can highlight the isospin diffusion effect, bypassing the effects acting similarly on the four systems (F. Rami et al., Phys. Rev. Lett. 84, 1120 (2000))

$$R(x) = \frac{2x_i - x_{AA} - x_{BB}}{x_{AA} - x_{BB}}$$

$R(x) = \pm 1 \longrightarrow$ non equilibrated

$R(x_{AB}) = R(x_{BA}) \longrightarrow$ full equilibration

where $A = {}^{64}$Ni, $B = {}^{58}$Ni, $i = AA, AB, BA, BB$ and x is an isospin sensitive observable.

Model-independent isospin transport ratio R(⟨N/Z⟩) for the QP remnant as a function of the impact parameter b

Regular behavior towards equilibration for increasing centralities (full equilibration is not achieved).

Experimental result providing a reference for comparison with theoretical predictions from transport models.
C. Ciampi *et al.*, Phys. Rev. C 111, 044601 (2025)

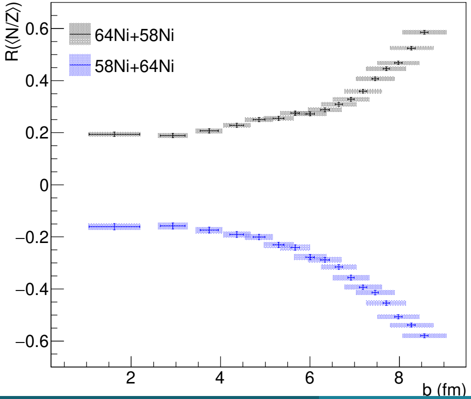

Extract information on **symmetry energy term** of nuclear EoS ← INDRA-FAZIA experimental data ← BUU@VECC-McGill calculations

Compare the experimental isospin transport ratio with the one predicted for *primary fragments* by the transport code:

- Avoid spurious effect from afterburner coupling
- Exploit i.t.r. property of largely suppressing the effects of statistical deexcitation

A. Camaiani *et al.*, Phys. Rev. C 102, 044607 (2020), S. Mallik *et al.*, J. Phys. G 49, 015102 (2021)

Simulations carried out with the BUU@VECC-McGill transport code:

S. Mallik *et al.*, Phys. Rev. C 91, 034616 (2015)

- BUU code, setting 100 test particles/nucleon
- 8 impact parameters for each reaction/parametrization
- 200 events for each impact parameter/reaction/parametrization
- Simulation run until 300fm/c (ITR convergence)
- Possibility to plug in and test different nEoS via metamodeling technique

J. Margueron *et al.*, Phys. Rev. C 97, 025805 (2018)

NEoS parametrizations from *ab initio* and phenomenological approaches:

- *Ab initio*:two extreme χ-EFT interactions from C. Drischler *et al.*, Phys. Rev. C 93, 054314 (2016)
- Phenomenological approaches:
  - SAMI (Skyrme), X. Roca-Maza *et al.*, Phys. Rev. C 86, 031306(R) (2012)
  - SGII (Skyrme), Nguyen Van Giai *et al.*, Phys. Lett. B106, 379 (1981)
  - NL3 (RMF), G. A. Lalazissis *et al.*, Phys. Rev. C 55, 540 (1997)

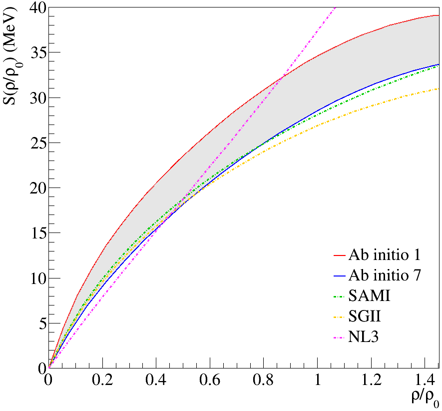

	n_{sat} (fm^{-3})	E_{sat} (MeV)	E_{sym} (MeV)	L_{sym} (MeV)	K_{sat} (MeV)	K_{sym} (MeV)
Ab initio 1	0.189	-16.92	34.57	48.5	241	224
Ab initio 7	0.140	-13.23	28.53	43.9	43.9	-144
SAMI	0.1587	-15.93	28.16	43.7	245	-120
SGII	0.1583	-15.59	26.83	37.6	215	-146
NL3	0.1480	-16.24	37.35	118.3	271	101

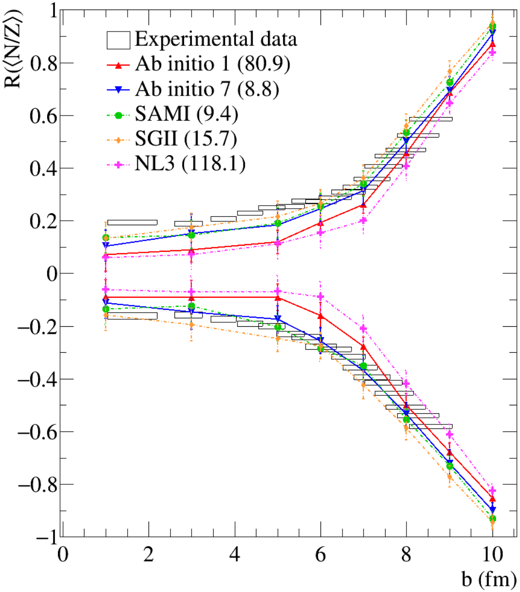

A few observations:

- SAMI vs *ab initio 7*: similar symmetry energy, different isoscalar behavior. Similar ITR indicates we are probing E_{sym}.
- NL3, *ab initio 1* → bad match: largest E_{sym} values above $0.5\rho_0$ can be excluded.
- SAMI, SGII, *ab initio 7* → good match: they feature similar E_{sym} values above $0.5\rho_0$

χ^2 values calculated by interpolating between the simulated data points:

	AI1	AI7	SAMI	SGII	NL3
χ^2	80.9	8.8	9.4	15.7	118.1

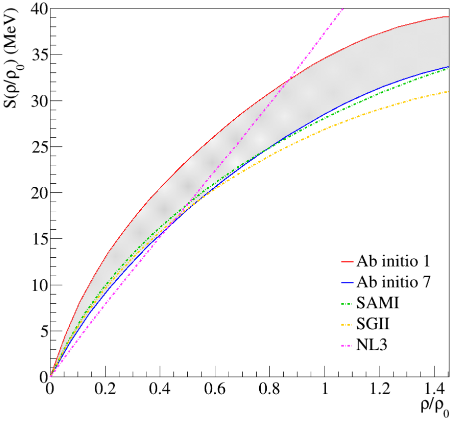

$S(\rho/\rho_0)$ (MeV)
ρ/ρ_0
0
5
10
15
20
25
30
35
40
0
0.2
0.4
0.6
0.8
1
1.2
1.4
Ab initio 1
Ab initio 7
SAMI
SGII
NL3

At each value of ρ/ρ_0:

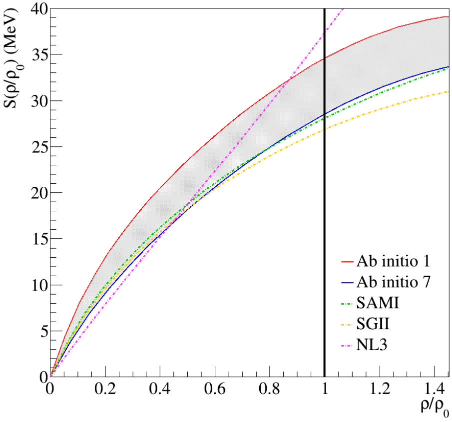

At each value of ρ/ρ_0:

- Pick $S(\rho/\rho_0)$ values corresponding to the 5 nEoS parametrizations

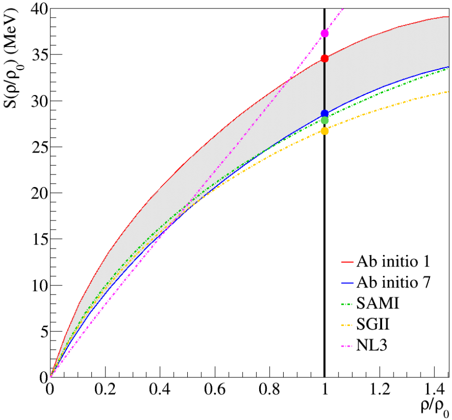

At each value of ρ/ρ_0:

- Pick $S(\rho/\rho_0)$ values corresponding to the 5 nEoS parametrizations
- Plot the 5 χ^2 values as a function of the $S(\rho/\rho_0)$ for the corresponding nEoS

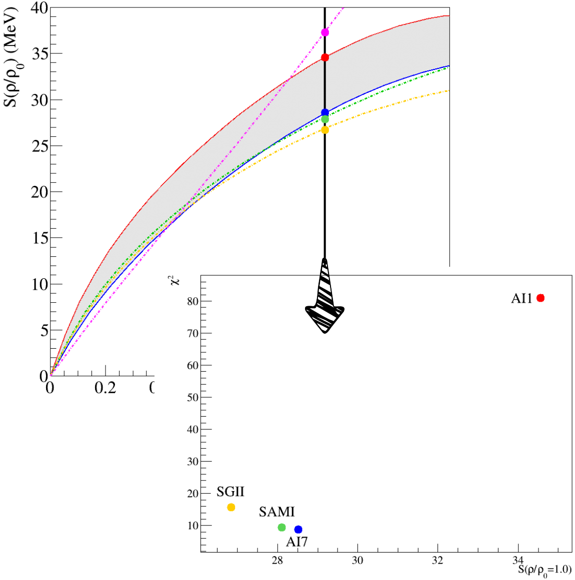

At each value of ρ/ρ_0:

- Pick $S(\rho/\rho_0)$ values corresponding to the 5 nEoS parametrizations
- Plot the 5 χ^2 values as a function of the $S(\rho/\rho_0)$ for the corresponding nEoS
- Quadratic fit to extract the parabolic dependence $\chi^2(S(\rho/\rho_0))$ around its minimum

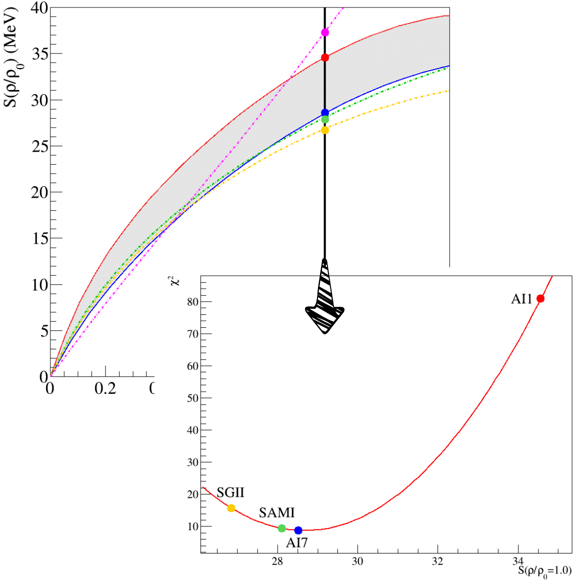

At each value of ρ/ρ_0:

- Pick $S(\rho/\rho_0)$ values corresponding to the 5 nEoS parametrizations
- Plot the 5 χ^2 values as a function of the $S(\rho/\rho_0)$ for the corresponding nEoS
- Quadratic fit to extract the parabolic dependence $\chi^2(S(\rho/\rho_0))$ around its minimum

Repeat along the ρ/ρ_0 axis.

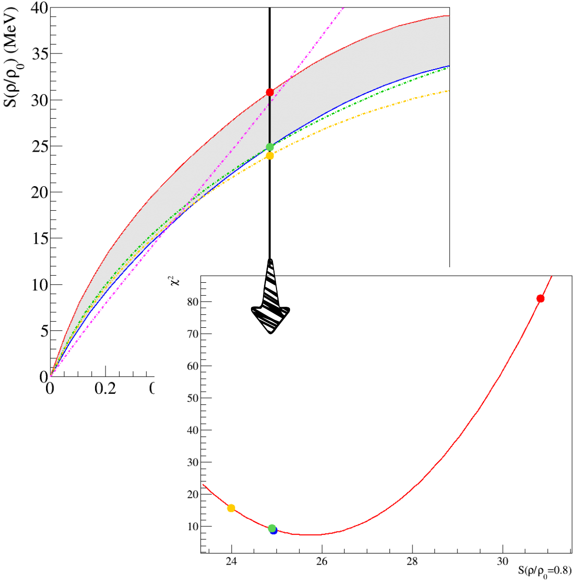

At each ρ/ρ_0 we thus define a likelihood along $\chi^2(S(\rho/\rho_0))$ as:

$$\mathcal{L}(S(\rho/\rho_0)) \propto e^{-\chi^2(S(\rho/\rho_0))/2}$$

→ extract the $N\sigma$ confidence intervals for $S(\rho/\rho_0)$
→ build approximate confidence region in the $S - \rho/\rho_0$ plane.

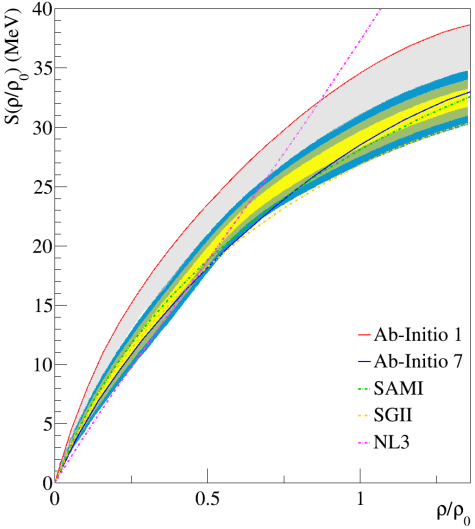

At each ρ/ρ_0 we thus define a likelihood along $\chi^2(S(\rho/\rho_0))$ as:

$$\mathcal{L}(S(\rho/\rho_0)) \propto e^{-\chi^2(S(\rho/\rho_0))/2}$$

→ extract the $N\sigma$ confidence intervals for $S(\rho/\rho_0)$
→ build approximate confidence region in the $S - \rho/\rho_0$ plane.

For a meaningful constraint we take into account the density region probed by the isospin diffusion phenomenon
→ define a *weight function*

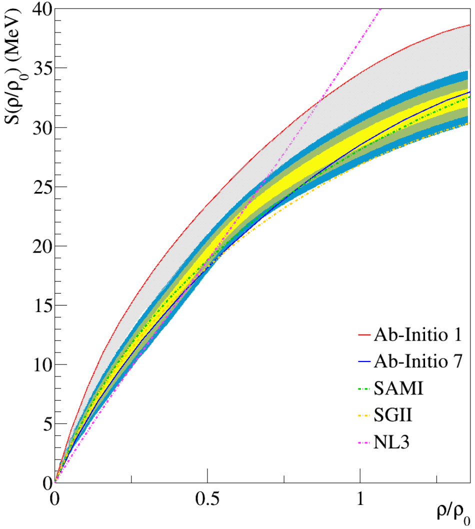

Study of the evolution of **baryonic density** and **isospin current density** extracted from BUU@VECC-McGill

- *Ab initio* 7 nEoS
- 200 events for 4 selected impact parameters ($b = 3, 5, 7, 9$ fm)
- Quantities evaluated over spherical volume with $r = 3$ fm
- n/p current densities evaluated along *principal axis*

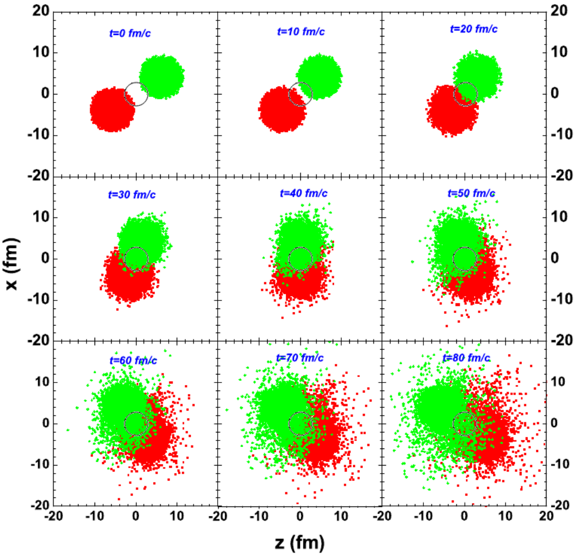

Study of the evolution of **baryonic density** and **isospin current density** extracted from BUU@VECC-McGill

- *Ab initio 7* nEoS
- 200 events for 4 selected impact parameters ($b = 3, 5, 7, 9$ fm)
- Quantities evaluated over spherical volume with $r = 3$ fm
- n/p current densities evaluated along *principal axis*

N.B. maximum exchange found in the compression phase, when the highest densities are reached.

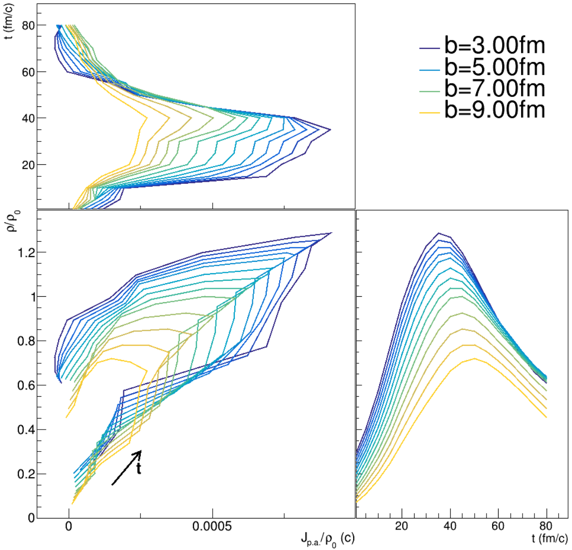

Weight function for a given impact parameter $w_b(\rho/\rho_0)$:

built as baryonic density cumulated over time, weighted by the corresponding current density

$$w_b(\rho/\rho_0) = \int_{t_{\text{start}}}^{t_{\text{stop}}} j_{\text{p.a.}}(t)\, \delta(\rho/\rho_0 - \rho(t)/\rho_0)\, dt$$

$\longrightarrow$ evaluated between 0 and 80 fm/c

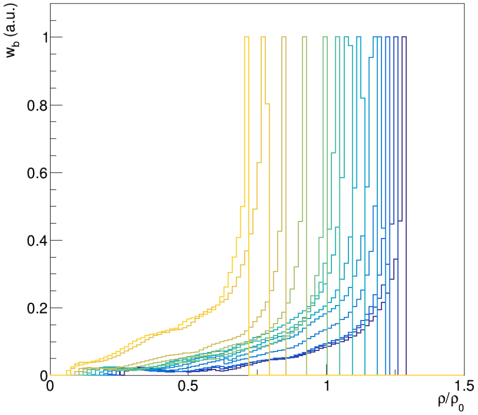

Weight function for a given impact parameter $w_b(\rho/\rho_0)$:

built as baryonic density cumulated over time, weighted by the corresponding current density

$$w_b(\rho/\rho_0) = \int_{t_{\rm start}}^{t_{\rm stop}} j_{\rm p.a.}(t)\,\delta(\rho/\rho_0 - \rho(t)/\rho_0)\,dt$$

→ evaluated between 0 and 80 fm/c

Global weight function $w(\rho/\rho_0)$:

$$w(\rho/\rho_0) = \int_{b_{\rm min}}^{b_{\rm max}} \tilde{w}_b(\rho/\rho_0)\,db$$

→ b interval between 3 and 9 fm

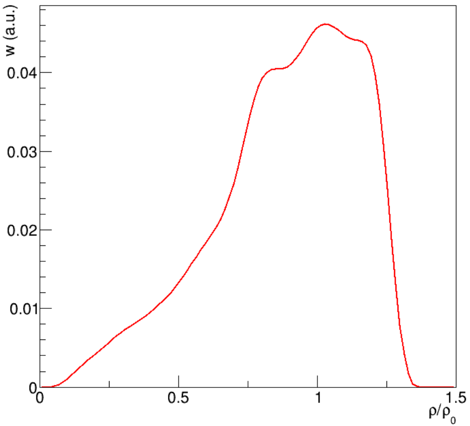

Confidence regions $1\sigma, 2\sigma, 3\sigma$ defined based on weighted $\mathcal{L}(S(\rho/\rho_0))$:

- Sensitivity close to saturation - anticipated by NL3 rejection, different from SAMI, SGII, AI7 for $\rho > 0.5\rho_0$

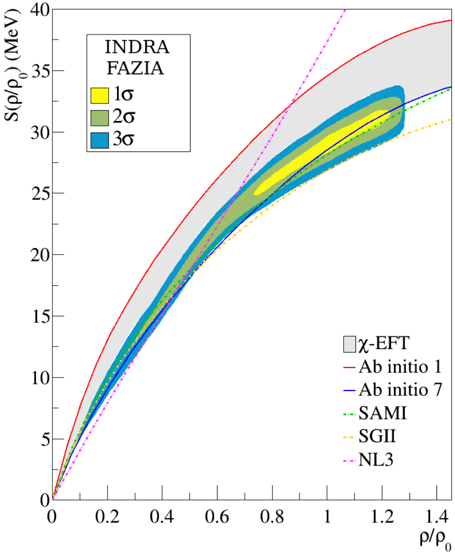

C. Ciampi *et al.*, Phys. Lett. B 868 (2025) 139815

Confidence regions $1\sigma, 2\sigma, 3\sigma$ defined based on weighted $\mathcal{L}(S(\rho/\rho_0))$:

- Sensitivity close to saturation - anticipated by NL3 rejection, different from SAMI, SGII, AI7 for $\rho > 0.5\rho_0$
- Good agreement with χ-EFT - towards the softer side of its uncertainty band

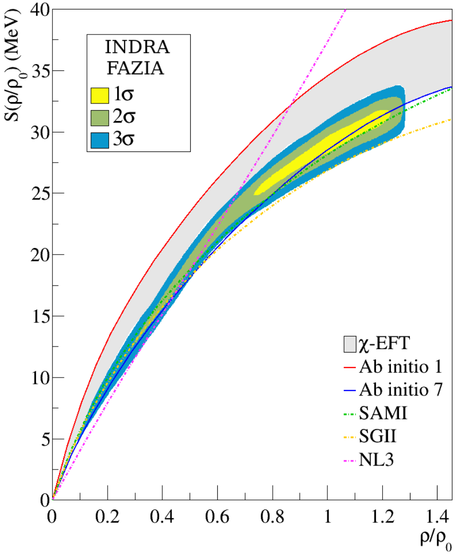

C. Ciampi *et al.*, Phys. Lett. B 868 (2025) 139815

Confidence regions $1\sigma, 2\sigma, 3\sigma$ defined based on weighted $\mathcal{L}(S(\rho/\rho_0))$:

- Sensitivity close to saturation - anticipated by NL3 rejection, different from SAMI, SGII, AI7 for $\rho > 0.5\rho_0$
- Good agreement with χ-EFT - towards the softer side of its uncertainty band
- Good agreement with isospin diffusion data in Sn+Sn collisions - (but we declare a different ρ sensitivity)

W. G. Lynch *et al.*, Phys. Lett. B 830, 137098 (2022).
M. B. Tsang *et al.*, Phys. Rev. Lett. 102, 122701 (2009).
P. Morfouace *et al.*, Phys. Lett. B 799, 135045 (2019).
Z. Zhang *et al.*, Phys. Rev. C 92, 031301R (2015).
M. Kortelainen *et al.*, Phys. Rev. C 85, 024304 (2012).
P. Danielewicz *et al.*, Nucl. Phys. A 958, 147 (2017).
B. T. Reed *et al.*, Phys. Rev. Lett. 126, 172503 (2021).

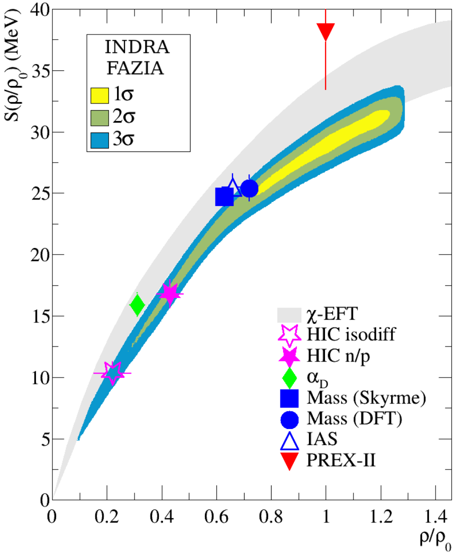

C. Ciampi *et al.*, Phys. Lett. B 868 (2025) 139815

Summary and conclusions

A new nuclear EoS constraint from isospin diffusion data:

- Comparison of model-independent experimentally-measured isospin transport ratio in $^{58,64}Ni+^{58,64}Ni$ collisions at 32 MeV/nucleon with the predictions of BUU@VECC-McGill transport model.
- EoS from both *ab initio* and phenomenological approaches considered.
- Consistent study of the time dependence of the baryonic density and of the isospin current density for the determination of the density region probed by the experiment.

Summary and conclusions

A new nuclear EoS constraint from isospin diffusion data:

- Comparison of model-independent experimentally-measured isospin transport ratio in ^{58,64}Ni+^{58,64}Ni collisions at 32 MeV/nucleon with the predictions of BUU@VECC-McGill transport model.
- EoS from both *ab initio* and phenomenological approaches considered.
- Consistent study of the time dependence of the baryonic density and of the isospin current density for the determination of the density region probed by the experiment.

Thank you!

C. Ciampi, S. Mallik, F. Gulminelli, D. Gruyer, J. D. Frankland, N. Le Neindre, R. Bougault, A. Chbihi, L. Baldesi, S. Barlini, B. Borderie, A. Camaiani, G. Casini, I. Dekhissi, J. A. Dueñas, Q. Fable, F. Gramegna, M. Henri, B. Hong, S. Kim, A. Kordyasz, T. Kozik, I. Lombardo, O. Lopez, T. Marchi, S. H. Nam, J. Park, M. Pârlog, G. Pasquali, S. Piantelli, G. Poggi, S. Valdré, G. Verde, E. Vient

INDRA FAZIA

Backup slides

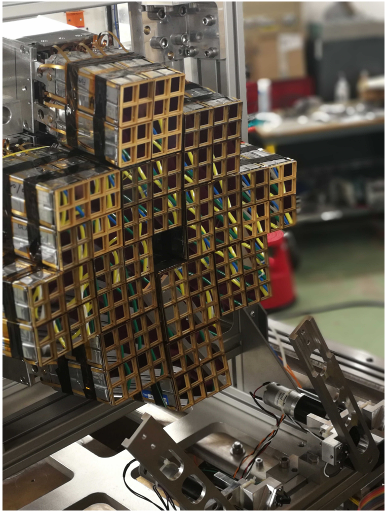

FAZIA *(Forward-angle A and Z Identification Array)*: optimal ion identification in the Fermi energy domain.

- Result of R&D activities to refine:
  - detector performance
  - digital treatment of signals
- Basic module: **block**, consisting of 16 three stage **telescopes** ($2 \times 2\,\mathrm{cm}^2$ active area):
  - Si1 300 μm thick
  - Si2 500 μm thick
  - CsI(Tl) 10cm thick

  \+ read-out electronics for all telescopes.
- Identification techniques: ΔE-E / PSA
  - Charge discrimination tested up to $Z \sim 55$
  - Mass discrimination up to $Z \sim 25$ / $Z \sim 22$

R. Bougault et al., Eur. Phys. J. A 50, 47 (2014)
S. Valdré et al., NIMA 930, 27 (2019)

INDRA *(Identification de Noyaux et Détection avec Résolutions Accrues)*: highly segmented array for detection and identification of charged products of heavy ion collisions at intermediate energies ($10 < E < 100$ AMeV).

- Original configuration of 17 rings:
  - 1: Phoswich detectors
  - 2-9: Ionisation ch. + Si + CsI(Tl)
  - 10-17: Ionisation ch. + CsI(Tl)
- Charge discrimination up to uranium, mass discrimination up to $Z \sim 4$
  → Electronics upgrade (2020): now up to $Z \sim 10$
  J. D. Frankland et al., Nuovo Cim. C 45, 43 (2022)

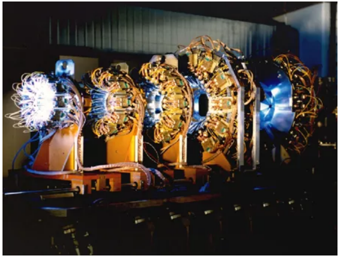

- Large solid angle coverage (90%) with high granularity (336 modules)

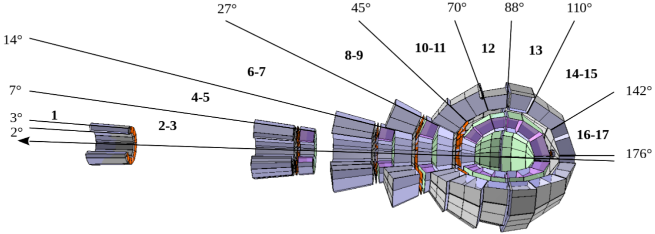

Here we present a combined analysis of two datasets of Ni-Ni collisions at 32 MeV/nucleon bearing complementary information:

Here we present a combined analysis of two datasets of Ni-Ni collisions at 32 MeV/nucleon bearing complementary information:

INDRA-FAZIA dataset $\rightarrow$ ^{58,64}Ni+^{58,64}Ni at 32 MeV/nucl.
Includes the information on the *isospin content of the QP remnant*.
Exp. aimed to study the **isospin diffusion mechanism** by comparing the products of the two asymmetric reactions with both the n-rich and n-deficient symmetric systems

Here we present a combined analysis of two datasets of Ni-Ni collisions at 32 MeV/nucleon bearing complementary information:

INDRA-FAZIA dataset → ^{58,64}Ni+^{58,64}Ni at 32 MeV/nucl.
Includes the information on the *isospin content of the QP remnant*.
Exp. aimed to study the **isospin diffusion mechanism** by comparing the products of the two asymmetric reactions with both the n-rich and n-deficient symmetric systems

- Trigger condition: $M_{\mathrm{FAZIA}} \geq 1$

Some events are discarded in a non-trivial way, especially for semiperipheral collisions.
The triangular $P(b)$ distribution does not well represent the experimental one.

Here we present a combined analysis of two datasets of Ni-Ni collisions at 32 MeV/nucleon bearing complementary information:

INDRA-FAZIA dataset → ^{58,64}Ni+^{58,64}Ni at 32 MeV/nucl.
Includes the information on the *isospin content of the QP remnant*.
Exp. aimed to study the **isospin diffusion mechanism** by comparing the products of the two asymmetric reactions with both the n-rich and n-deficient symmetric systems

- Trigger condition: $M_{\text{FAZIA}} \geq 1$

Some events are discarded in a non-trivial way, especially for semiperipheral collisions.
The triangular $P(b)$ distribution does not well represent the experimental one.

INDRA dataset → ^{58}Ni+^{58}Ni at 32 MeV/nucl.

- Trigger condition: $M_{\text{tot}} \geq 4$

Minimum bias, the $P(b)$ can be well approximated as shown before (with $\Delta b \approx 0.4$fm). (see J. D. Frankland et al., Phys. Rev. C 104, 034609 (2021), E. Vient et al., Phys. Rev. C 98, 044612 (2018))
Suitable for the application of the *impact parameter reconstruction method*.

Procedure for the reaction in common ^{58}Ni+^{58}Ni at 32 MeV/nucl.:

1. Centrality estimation on "unbiased" INDRA dataset
2. Apply $X - b$ relationship to INDRA-FAZIA dataset

Procedure for the reaction in common ^{58}Ni+^{58}Ni at 32 MeV/nucl.:

1. Centrality estimation on "unbiased" INDRA dataset
2. Apply $X - b$ relationship to INDRA-FAZIA dataset

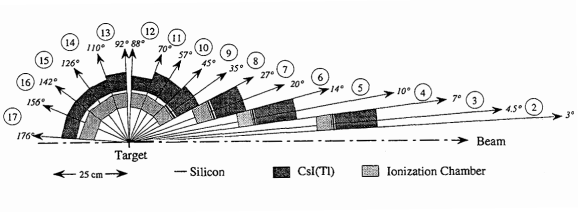

Procedure for the reaction in common $^{58}Ni+^{58}Ni$ at 32 MeV/nucl.:

1. Centrality estimation on "unbiased" INDRA dataset
2. Apply $X-b$ relationship to INDRA-FAZIA dataset

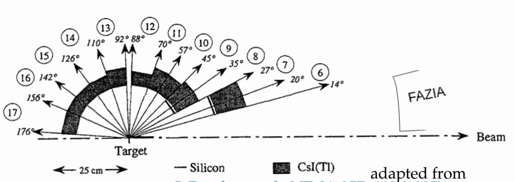

adapted from
J. Pouthas et al., NIMA 357, 418 (1995)

Procedure for the reaction in common ^{58}Ni+^{58}Ni at 32 MeV/nucl.:

1. Centrality estimation on "unbiased" INDRA dataset
2. Apply $X - b$ relationship to INDRA-FAZIA dataset

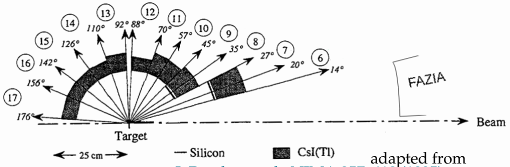

adapted from J. Pouthas et al., NIMA 357, 418 (1995)

Centrality observable X

multiplicity M of *identified* and *unidentified* particles in INDRA rings 6 to 17.

Procedure for the reaction in common ^{58}Ni+^{58}Ni at 32 MeV/nucl.:

1. Centrality estimation on "unbiased" INDRA dataset
2. Apply $X-b$ relationship to INDRA-FAZIA dataset

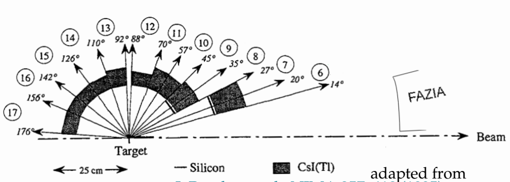

adapted from J. Pouthas et al., NIMA 357, 418 (1995)

Centrality observable X

multiplicity M of *identified* and *unidentified* particles in INDRA rings 6 to 17.

Procedure for the other systems:

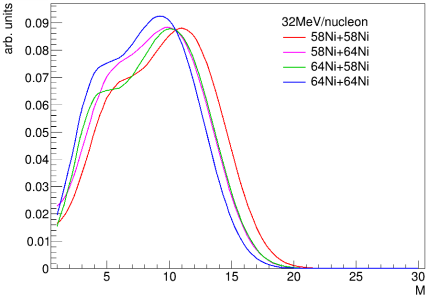

Procedure for the reaction in common ^{58}Ni+^{58}Ni at 32 MeV/nucl.:

1. Centrality estimation on "unbiased" INDRA dataset
2. Apply $X - b$ relationship to INDRA-FAZIA dataset

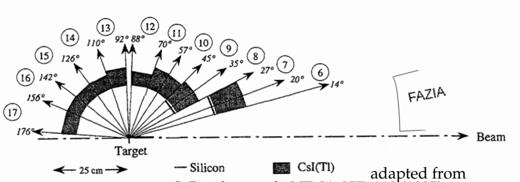

adapted from J. Pouthas et al., NIMA 357, 418 (1995)

Centrality observable X

multiplicity M of *identified* and *unidentified* particles in INDRA rings 6 to 17.

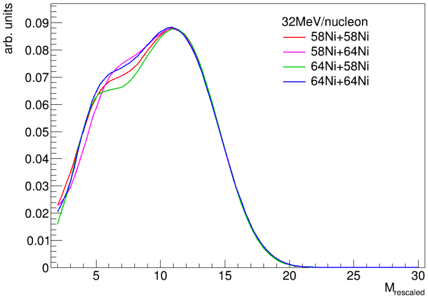

Procedure for the other systems:

→ rescale the detected multiplicity M_{sys} into a corresponding M_{resc} value for ^{58}Ni+^{58}Ni.

$$M_{resc} = \lfloor \alpha \cdot (M_{sys} + r) + \beta \rfloor$$

where $r \sim U([0,1])$ is a uniformly distributed random variable taking values in $[0, 1]$.

Outline

Absolute b distributions → set $P(b)$ parameters in a model independent way:

$$P(b) = \frac{2\pi b}{1+\exp[(b-b_0)/\Delta b]}$$

$\Delta \mathbf{b} \approx$ **0.4 fm** as verified in PRC 104, 034609 (2021)

$\mathbf{b_0}$ by inverting $\sigma_R = -2\pi(\Delta b)^2 \mathrm{Li}_2\left[-\exp\left(\frac{\mathbf{b_0}}{\Delta b}\right)\right]$

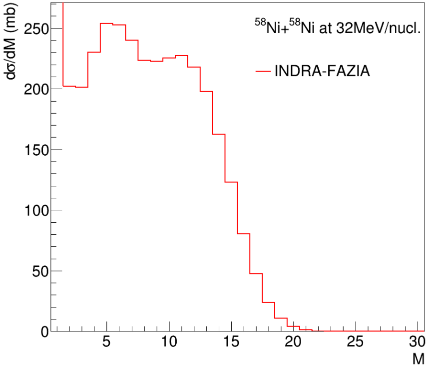

For the estimation of σ_R, and hence b_0:

- Use the elastic scattering events in the INDRA-FAZIA dataset ($M_{FAZIA} \geq 1$) as reference for cross section normalization

Absolute b distributions $\rightarrow$ set $P(b)$ parameters in a model independent way:

$$P(b) = \frac{2\pi b}{1+\exp[(b-b_0)/\Delta b]}$$

- $\mathbf{\Delta b \approx 0.4}$ **fm** as verified in PRC 104, 034609 (2021)
- $\mathbf{b_0}$ by inverting $\sigma_R = -2\pi(\Delta b)^2 \mathrm{Li}_2\left[-\exp\left(\frac{\mathbf{b_0}}{\Delta b}\right)\right]$

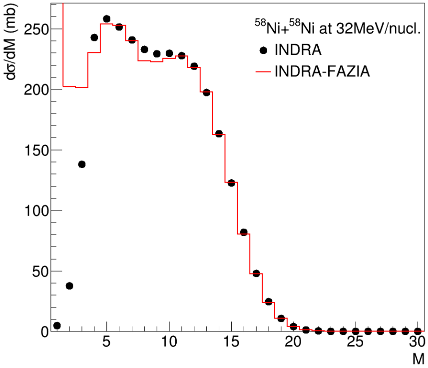

For the estimation of σ_R, and hence b_0:

- Use the elastic scattering events in the INDRA-FAZIA dataset ($M_{FAZIA} \geq 1$) as reference for cross section normalization
- Transfer the normalization to the INDRA dataset using the high multiplicity tail, after correcting for small trigger effect
  $\rightarrow \sigma_R$ INDRA dataset $\Rightarrow b_0 = (9.8 \pm 0.7)$ fm

Absolute b distributions → set $P(b)$ parameters in a model independent way:

$$P(b) = \frac{2\pi b}{1+\exp[(b-b_0)/\Delta b]}$$

- $\mathbf{\Delta b} \approx \mathbf{0.4\ fm}$ as verified in PRC 104, 034609 (2021)
- $\mathbf{b_0}$ by inverting $\sigma_R = -2\pi(\Delta b)^2 \mathrm{Li}_2\left[-\exp\left(\frac{\mathbf{b_0}}{\Delta b}\right)\right]$

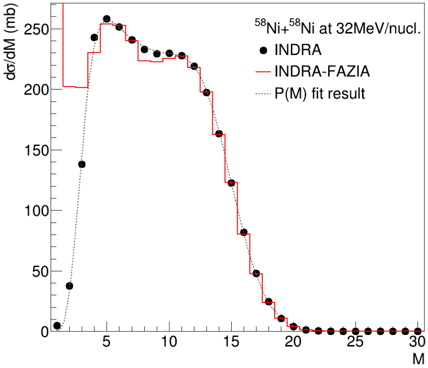

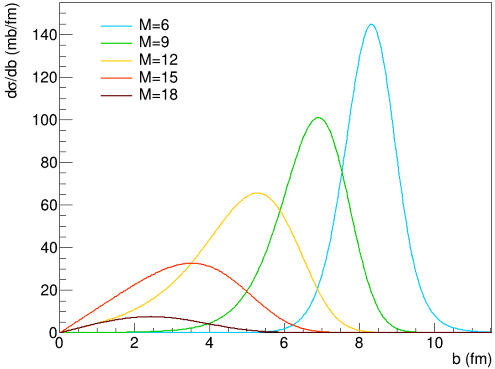

→ important role of **intrinsic fluctuations**: relatively different M selections populate partly (or entirely) superimposed b intervals

Study of the evolution of **baryonic density** and **isospin current density** extracted from BUU@VECC-McGill

- *Ab initio 7* nEoS
- 200 events for 4 selected impact parameters ($b = 3, 5, 7, 9$ fm)
- Quantities evaluated over spherical volume with $r = 3$ fm

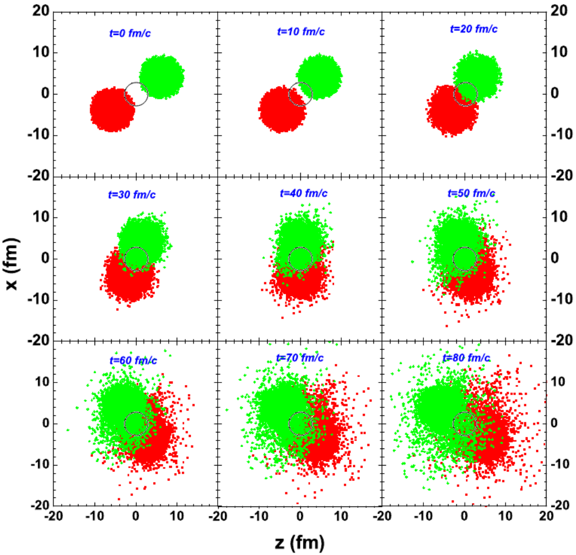

Study of the evolution of **baryonic density** and **isospin current density** extracted from BUU@VECC-McGill

- *Ab initio 7* nEoS
- 200 events for 4 selected impact parameters ($b = 3, 5, 7, 9$ fm)
- Quantities evaluated over spherical volume with $r = 3$ fm

Principal axis extracted at each timestep by diagonalizing the momentum of inertia tensor.
Current densities evaluated in its reference frame.

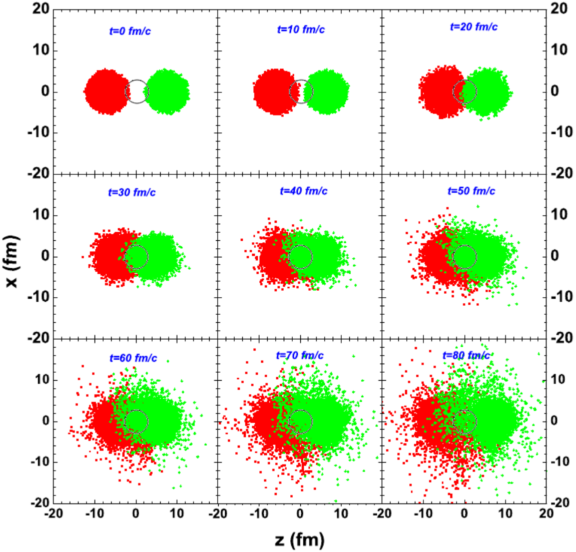

The values of baryonic density and isospin current density depend on the radius of the spherical volume used for their evaluation.

- For $r > 3$ fm the sphere extends beyond the neck region (including empty areas), which reduces both the density and the current density
- For $r < 3$ fm, the finite number of test particles within the sphere introduces strong statistical fluctuations that affect the current evaluation

The radius equal to 3 fm has been chosen as the optimal value, balancing these competing effects.

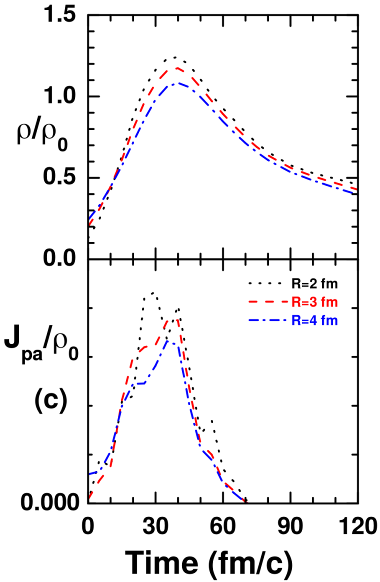

n/p current densities evaluated as:

$$\vec{j}_q^{(X)} = \frac{1}{V}\int_V d^3 r \rho_q^{(X)}(\vec{r})\vec{v}_q^{(X)}(\vec{r}).$$

Nucleon exchange determined by $\vec{j}_q^{(X)}$ components along the principal axis.

Net isospin current density obtained as the difference between neutron and proton current densities.

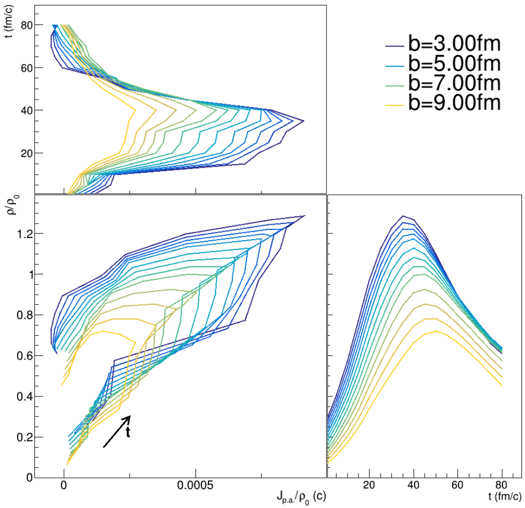

n/p current densities evaluated as:

$$\vec{j}_q^{(X)} = \frac{1}{V}\int_V d^3r\rho_q^{(X)}(\vec{r})\vec{v}_q^{(X)}(\vec{r}).$$

Nucleon exchange determined by $\vec{j}_q^{(X)}$ components along the principal axis.

Net isospin current density obtained as the difference between neutron and proton current densities.

N.B. maximum exchange found in the compression phase, when the highest densities are reached.

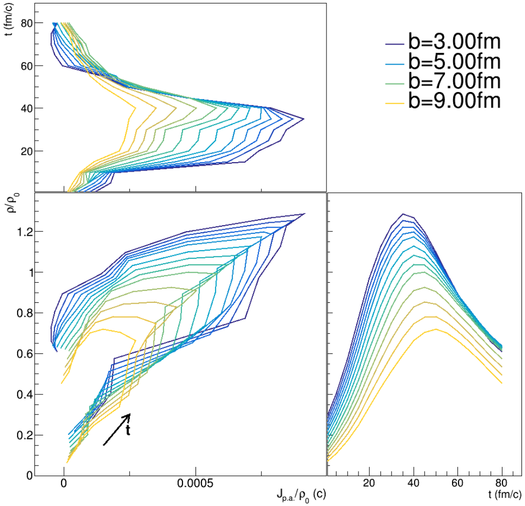

The confidence regions slightly depend on the choice of b and t intervals for the weight function, but our observations are stable against these arbitrary choices.

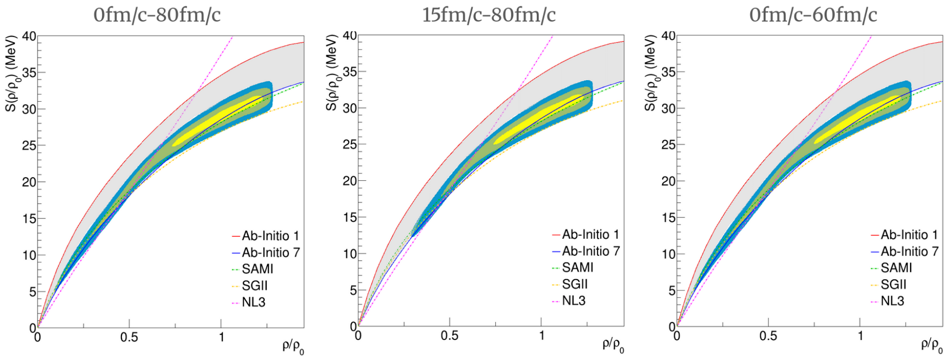

e.g., varying the time interval for the weight function evaluation essentially changes the contribution from the low density tail.

Physical information is obtained by comparing experimental results and transport model simulations *assuming the same conditions*.

Impact parameter: experimentally, it can be only deduced from observables such as multiplicities, transverse energies, flow angle...

All physics observables are affected by **intrinsic fluctuations** associated with the underlying processes.
Such fluctuations can limit the accuracy in treating centrality and bias the comparisons with simulated data.
L. Li et al., PRC 97,044606 (2018), G. Q. Zhang et al., PRC 84, 034612 (2011)

Different approaches for reaction centrality characterization:

- Sharp cutoff approximation C. Cavata et al., Phys. Rev. C 42, 1760 (1990)
- Machine learning algorithms trained on simulations
  F. Li et al., PRC 104,034608 (2021), F. Haddad et al., PRC 55, 1371 (1997)
- **Model-independent** method to reconstruct impact parameter distributions → includes **fluctuations**
  J. D. Frankland et al., PRC104, 034609 (2021), R. Rogly et al., PRC98, 024902 (2018)

Given a centrality observable X, its inclusive distribution $P(X)$ can be expressed as:

$$P(X) = \int_0^\infty P(X,b)\,db = \int_0^\infty P(b)\,P(X|b)\,db = \int_0^1 P(X|c_b)\,dc_b$$

where a change of variables is applied, introducing the centrality $c_b \equiv \int_0^b P(b')\,db'$ and exploiting that $P(c_b) = 1$.

Key step: model the $P(X|c_b)$ and extract its parameters by fitting the experimental $P(X)$ X assumes positive values → non-negative gamma distribution as fluctuation kernel:

$$P(X|c_b) = \frac{1}{\Gamma(k)\theta^k} X^{k-1} e^{-X/\theta} \qquad \text{where } \bar{X} = k\theta \text{ and } \sigma_X = \sqrt{k}\theta$$

where k and θ generally evolve with centrality. For them we assume:

- $k(c_b) = k_{\max}[1 - c_b^\alpha]^\gamma + k_{\min}$, where α, γ, $k_{\min}$ and $k_{\max}$ are parameters of the fit
- θ independent of centrality (problem is underconstrained) → θ is a fit parameter

Once the $P(X|c_b)$ is determined, one obtains:

$$P\left(c_b|x_1 \le X \le x_2\right) = \frac{\int_{x_1}^{x_2} P(c_b, X)\,dX}{\int_{x_1}^{x_2} P(X)\,dX} = \frac{\int_{x_1}^{x_2} P(X|c_b)\,dX}{\int_{x_1}^{x_2} P(X)\,dX}$$

and by changing back the variable: $P\left(b|x_1 \le X \le x_2\right) = P(b)\,P\left(c_b(b)|x_1 \le X \le x_2\right)$